How to cite: *Angew. Chem. Int. Ed.* **2025**, *64*, e202416058
doi.org/10.1002/anie.202416058

Solvatochromism

Nuclear Quantum Effects Have a Significant Impact on UV/Vis Absorption Spectra of Chromophores in Water

Shota Tsuru[+],* *Bikramjit Sharma*[+], *Christof Hättig, and Dominik Marx*

Abstract: Despite the broadly acknowledged importance of solvation effects on measured UV/Vis spectra in the context of solvatochromism or chemical reactions in solution, it is still an open challenge to calculate UV/Vis spectra with predictive accuracy. This is particularly true when it comes to the impact of nuclear quantum effects on these experimental observables. In the present work, we calculate the UV/Vis absorption spectrum of indole in aqueous solution with a combination of a correlated wavefunction method for computing electronic excitation energies and enhanced path integral simulations for rigorous sampling of nuclear configurations including the quantum effects in solution. After validating our approach based on gas-phase benchmarking, we demonstrate that the lineshape of the spectrum measured in aqueous solution is quantitatively recovered, without the application of any shifting, scaling, or broadening, only after including nuclear quantum effects in addition to thermal fluctuations and solvation at ambient conditions. Our findings demonstrate that nuclear quantum effects are "visible" in UV/Vis spectra of chromophores measured in solution even at room temperature and, therefore, that they must be considered computationally to achieve predictive accuracy.

The significant solvent influence on spectra, as evidenced by solvatochromism, has been recognized for centuries,[1,2] yet it continues to be a subject of intense research.[3–17] More recently, the development of time-resolved spectroscopies greatly extended the possibility of microscopic investigations toward dynamical solvent effects.[18–30] In parallel to experiments, significant advances have been achieved in electronic structure-based computational spectroscopy of molecular solutions, including work that takes classical thermal fluctuations into account.[31–44] The importance of including nuclear quantum effects (NQEs) in calculations is well documented for spectroscopic properties of molecular systems in the gas phase.[45–47] When it comes to the impact of NQEs on electronic spectra in solutions, there are a few reports in the literature which studied their role through simulation approaches. Most of them used ensemble approaches, where the vibrational effects were explicitly considered,[48–56] whereas others used dynamical lineshape approaches, where the lineshapes were calculated for each snapshot considering vibronic effects.[57–59] All of them reproduced the widths of bands in measured spectra better by considering NQEs, as expected from the well-known impact of NQEs on the structural dynamics of water and aqueous solutions.[60] Nevertheless, a thorough investigation of the solvent influence on spectra, especially contribution of NQEs to solvatochromism, comparing directly with spectra measured both in the gas phase and in solution, has not yet been accomplished.

In this Letter, we evaluate and quantify the combined impact of NQEs and solvation on the UV/Vis absorption spectrum of indole in water with reference to the gas phase where reliable experimental benchmark spectra are available. We select indole (see Figure 1) not only due to its broad multidisciplinary interest[61–69] but also in view of its clearly observed solvatochromism[70,71] and the considerable interest in its photoinduced dynamics both in the gas phase[70,72–74] and in neutral aqueous solution.[71] Moreover, indole is a quasi-rigid molecule and amenable to well-established Wigner sampling of NQEs based on the harmonic approximation in the gas phase.[33,46,47] In the gas phase, this allows for one-to-one comparisons between Wigner sampling and the same rigorous ab initio simulation methodology[75] (namely path integral quantum thermal bath (PIQTB) simulations[76,77]), which can also be used in

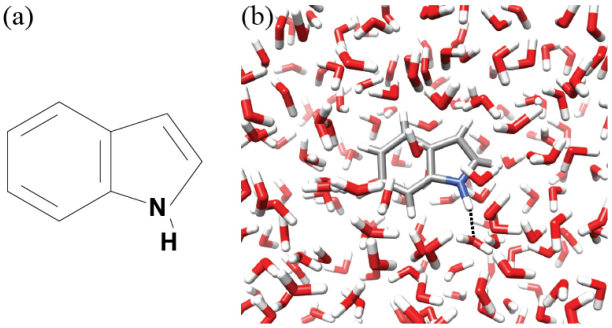


Figure 1. (a) Schematic structure of indole. (b) Solvation structure of indole in water. The dashed line indicates the hydrogen bond between the N–H group and a water molecule.

[*] Dr. S. Tsuru,[+] Dr. B. Sharma,[+] Prof. Dr. C. Hättig, Prof. Dr. D. Marx
Lehrstuhl für Theoretische Chemie
Ruhr-Universität Bochum
44780 Bochum, Germany
Dr. S. Tsuru[+]
RIKEN Center for Computational Science
Minatojima-minami 7-1-26
650-0047, Kobe, Japan
E-mail: shota.tsuru@riken.jp
[+] These authors contributed equally.

© 2024 Wiley-VCH GmbH

solutions to sample the combined effects due to solvation, temperature, and NQEs. This capability of the PIQTB simulation is a major advantage over Wigner sampling, which requires significant approximations when applied to practical finite-temperature simulations in solution. Combined with such quantum sampling, we use the accurate algebraic-diagrammatic construction through second order, ADC(2),[78–80] approach to compute electronic excitation energies without any need of artificial scaling or shifting.[81] Importantly, our quantum ensemble approach rigorously accounts for thermal as well as vibrational broadening effects, fully including state mixing and intensity borrowing along the ground-state vibrational modes in solution; vibronic effects such as those arising from the quantization of vibrational levels in excited states and Franck–Condon factors are not covered[45] but would be accessible using well-known dynamical lineshape approaches.[57–59] Concerning the methods used, we refer to the Supporting Information.

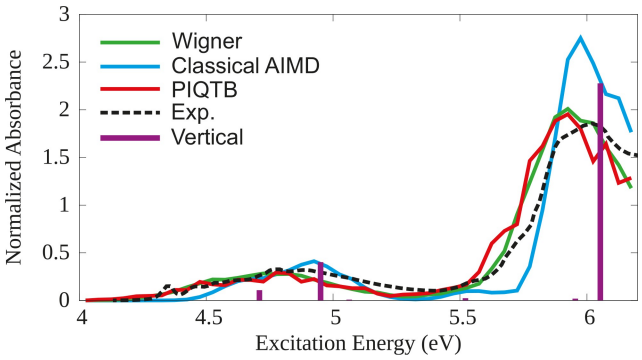


Figure 2. UV/Vis absorption spectrum of indole in the gas phase calculated based on Wigner sampling (green) as well as on canonical sampling from trajectories generated at 300 K using classical (AIMD: blue) and quantum (PIQTB: red) nuclei. The dashed black line is the corresponding measured spectrum digitized from Ref. [70]. The purple sticks indicate the vertical spectrum calculated at the optimized geometry of indole.

Table 1: Energies (in eV), oscillator strengths (OSs) and occupied (Occ.) as well as virtual (Vir.) natural transition orbitals (NTOs) for the vertical excitations up to 5.4 eV from the ground state of indole at the ground-state optimized geometry in the gas phase (NTO isosurface is 0.02 for Rydberg-type orbitals and 0.05 for others). The value of σ denotes the singular values for the NTO pairs and σ^2 provides the relative weight of each NTO pair in the excitation. See Table S1 for higher excitations.

	Energy	OS	Occ.	σ^2	Vir.
^1L_b	4.71	0.0300		0.73	
				0.26	
^1L_a	4.95	0.1118		0.92	
				0.07	
Ryd	5.06	0.0025		0.99	

Figure 2 shows the UV/Vis absorption spectrum of gas-phase indole calculated based on the classical AIMD (ab initio molecular dynamics), Wigner, and PIQTB samplings, compared one-to-one to the experimental benchmark.[70] The vertical excitation energies and the natural transition orbitals (NTOs)[82–85] calculated at the ground-state optimized geometry are given in Table 1. The combined absorption bands in the energy window of 4.2 to 5.4 eV originate from the two $^1\pi\pi^*$ states named ^1L_b and ^1L_a in accordance with Platt nomenclature.[86] The absorption bands above 5.4 eV, with intensity more than five times larger than that of the bands below 5.4 eV, originate from further $^1\pi\pi^*$ states. In this energy window, excited states like the third one in Table 1, where an electron is transferred to a Rydberg orbital, are also located. The close agreement between the gas-phase spectra of the quasi-rigid indole molecule calculated from Wigner and PIQTB samplings shown in Figure 2 explicitly demonstrates that the PIQTB sampling properly accounts for NQEs in the gas phase.

The spectrum calculated based on classical AIMD exhibits positions and intensities of the bands close to those of the vertical spectrum. More importantly, the classical spectrum does not reproduce the band shapes of the measured spectrum, although the positions of the maxima (4.93 and 5.98 eV) are somewhat close to the measured ones (4.88 and 6.02 eV). Meanwhile, the spectra calculated based on the Wigner and PIQTB samplings are broader than those based on the classical AIMD sampling and agree much better with the measured spectrum.

To quantify the NQEs on the excitation energies, we collect in Table 2 the results for the $S_1(^1L_b)$, $S_2(^1L_a)$, and S_3(Ryd) states calculated at the optimized geometry and those obtained as averages for the AIMD, PIQTB, and Wigner ensembles. For the classical AIMD ensemble, small red shifts, 0.06 and 0.03 eV, are obtained for the S_1 and S_2 states, respectively. For the PIQTB and Wigner ensembles, these shifts are as large as 0.17–0.18 and 0.11–0.13 eV for S_1 and S_2, respectively. In contrast to S_1 and S_2 dominated by the configurations of $^1\pi\pi^*$ character, a red shift of S_3 is observed only for the PIQTB and Wigner quantum ensembles. This can be explained by the configuration of Rydberg character which is insensitive to molecular distortions and, thereby, to NQEs. Similar shifts from including NQEs when sampling nuclear configurations were observed for other cases.[34] However, it should be noted that the

Table 2: Excitation energies (eV) of the $S_1(^1L_b)$, $S_2(^1L_a)$, and S_3(Ryd) states calculated at the optimized geometry (vertical) and those obtained as averages of vertical excitation energies calculated for the classical AIMD, PIQTB, and Wigner ensembles of indole in the gas phase.

	S_1	S_2	S_3
Vertical	4.71	4.95	5.06
Classical AIMD	4.65	4.92	5.06
PIQTB	4.53	4.84	5.04
Wigner	4.54	4.82	5.00

© 2024 Wiley-VCH GmbH

15213773, 2025, 3, Downloaded from https://onlinelibrary.wiley.com/doi/10.1002/anie.202416058 by Ruhr-Universität Bochum, Wiley Online Library on [05/03/2025]. See the Terms and Conditions (https://onlinelibrary.wiley.com/terms-and-conditions) on Wiley Online Library for rules of use; OA articles are governed by the applicable Creative Commons License

observed difference between the gas-phase spectra calculated with or without considering NQEs is specific not only to the molecular species, but also to the character of each electronic state: For the lowest spin-singlet excited states of pyrazine, the difference is limited to the width of the bands and the shift due to NQEs is not obvious.[43] Given the state-specificity of NQEs, one cannot account for quantum effects on UV/Vis absorption spectra even of a given molecule by a global shifting or scaling of the excitation energies, thus underlining the importance of explicit inclusion of NQEs in predictive computations as the present ones.

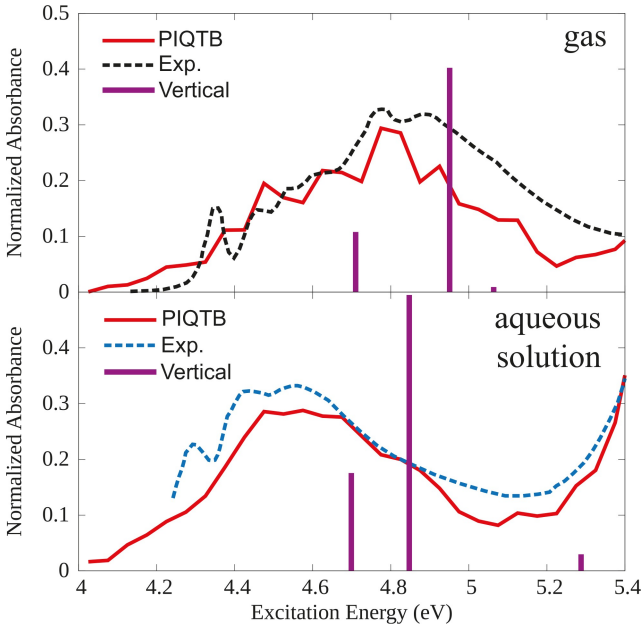


Figure 3. UV/Vis absorption spectra of indole in the gas phase (top) and in aqueous solution (bottom) calculated based on the canonical trajectories generated at 300 K representing quantum nuclei according to PIQTB sampling (red). Dashed black and blue lines are the corresponding measured spectra digitized from Refs. [70] and [71], respectively. The purple sticks indicate the vertical spectrum calculated at the optimized geometry of the isolated indole molecule (top) and in aqueous solution according to COSMO solvation (bottom), see text.

Table 3: Energies (eV), oscillator strengths (OSs) and occupied (Occ.) as well as virtual (Vir.) natural transition orbitals (NTOs) of the vertical excitations up to 5.4 eV from the ground state of indole at the ground-state optimized geometry in water according to COSMO solvation, see text (NTO isosurface is 0.02 for Rydberg-type orbitals and 0.05 for others). The value of σ denotes the singular values for the NTO pairs and σ^2 provides the relative weight of each NTO pair in the excitation. See Table S2 for higher excitations.

	Energy	OS	Occ.	σ^2	Vir.
^1L_b	4.70	0.0487		0.83	
				0.17	
^1L_a	4.85	0.1375		0.90	
				0.09	
Ryd	5.29	0.0083		0.99	

We now turn to the importance of NQEs in aqueous solution as well as the specific solvation effects on the excited states of the solute as seen in the UV/Vis absorption of indole in aqueous solution. Figure 3 shows the UV/Vis absorption spectra of indole in the gas phase and in aqueous solution calculated based on PIQTB sampling compared to the experimental benchmarks.[70,71] The vertical excitation energies and the NTOs calculated by embedding indole into the conductor-like screening model (COSMO)[87,88] at the ground-state optimized geometry are given in Table 3. The first sharp absorption at 4.36 eV (gas phase) and 4.30 eV (aqueous solution) in the measured spectra originates from the 0-0 component of the ^1L_b absorption band,[89] which is not accessible by ensemble approaches. The maxima of the combined absorption bands in the spectrum measured in aqueous solution (4.44 and 4.56 eV) experience more than 0.3 eV red shifts from those in the spectrum measured in the gas phase (4.79 and 4.88 eV), and the more intense absorption bands start to rise at 5.14 eV in aqueous solution while this happens only at 5.42 eV in the gas phase. Importantly, PIQTB sampling succeeds in reproducing not only the band maxima but also the width both in the gas phase and in aqueous solution, including the increase of the absorbance starting at 5.14 eV in aqueous solution, which was not examined previously.[51]

Next, to disentangle the specific solvation effects on the molecular and electronic structures appearing in the UV/Vis absorption spectrum, we first discuss the bulk solvation effects. We do this by examining the vertical spectrum calculated at the ground-state optimized geometry, embedding the indole molecule in COSMO (compare Tables 1 and 3). In the energy window of 4.0–5.4 eV, the $^1\pi\pi^*$ (^1L_b and ^1L_a) states experience up to a 0.1 eV red shift without change in the configuration characters. In contrast, $^1\pi$Ryd states experience more than a 0.2 eV blue shift with qualitative changes in the virtual NTOs. These effects observed in the vertical excitation do not fully account for the solvation effects in the UV/Vis absorption spectrum observed in Figure 3, since the shifts of the vertical excitation energies, up to 0.1 eV, are small compared to the band maxima shifts observed in the experiments, which are more than 0.3 eV.

We then compare the spectra calculated for the classical AIMD ensembles in the gas phase and in aqueous solution (see Figure S4). The band maximum of the spectrum calculated for the aqueous solution (4.78 eV) is lower than that of the spectrum calculated for the gas phase (4.93 eV) by 0.15 eV. This red shift observed in the spectra calculated for the classical AIMD ensembles is larger than that observed for the ^1L_a state in the single-point calculations, 0.10 eV. Table 4 shows the excitation energy of each state averaged for the classical AIMD ensemble (used for Figure S4) and the PIQTB ensemble (used for Figure 3) in aqueous solution. For the S_1 and S_2 states, the average excitation energies calculated for the classical AIMD ensemble are lower than those calculated at the optimized geometry by 0.09 and 0.05 eV, respectively. These differ-

© 2024 Wiley-VCH GmbH

15213773, 2025, 3, Downloaded from https://onlinelibrary.wiley.com/doi/10.1002/anie.202416058 by Ruhr-Universität Bochum, Wiley Online Library on [05/03/2025]. See the Terms and Conditions (https://onlinelibrary.wiley.com/terms-and-conditions) on Wiley Online Library for rules of use; OA articles are governed by the applicable Creative Commons License

Table 4: Excitation energies (eV) of the $S_1(^1L_b)$, $S_2(^1L_a)$, and S_3(Ryd) states calculated at the optimized geometry (vertical) and those obtained as averages of vertical excitation energies calculated for the classical AIMD and PIQTB ensembles of indole dissolved in water.

	S_1	S_2	S_3
Vertical	4.70	4.85	5.29
Classical AIMD	4.61	4.80	5.23
PIQTB	4.48	4.76	5.18

ences are larger than those in the gas phase (0.06 and 0.03 eV, see Table 2), indicating a contribution from thermal fluctuation of the solvent to the red shift. Nevertheless, the 0.15 eV shift of the band maximum is still too small in comparison to 0.32 eV observed in the experiments. Thus, distortions of the molecular skeleton of indole in solution caused by the interaction with solvent molecules obtained with classical thermal fluctuations generated by AIMD do not fully account for the solvation effects, either. In contrast, as seen in the upper and lower panels of Figure 3, the 0.20 eV shift of the band maximum obtained in the calculations based on PIQTB sampling from the gas phase (4.78 eV) to aqueous solution (4.58 eV) match the experimental shift much better. These results clearly indicate that the solvatochromic effects observed in experimental UV/Vis spectra are highly sensitive to NQEs!

Given these findings, let us now disentangle the distinct factors due to solvation that do—and do not—affect the calculated spectrum. Figure S6 presents the underlying full details by presenting the spectra obtained in the PIQTB ensemble of indole in bulk water calculated (i) without taking solvent into account at all when calculating the UV/Vis spectrum [PIQTB (no COSMO)], (ii) replacing all solvent molecules with continuum embedding [PIQTB (Indole + COSMO)], and (iii) replacing water with the COSMO continuum solvent except for those explicit water molecules that are within the hydrogen bonding region of the indole N–H group [PIQTB (Indole + Hbond H_2O + COSMO)]; only the spectrum obtained using the most accurate approach (iii) is shown in the bottom panel of Figure 3. We find that the shape of the absorption band is rectified even without considering the solvent molecules in the excited-state calculations, although the band maximum is still somewhat too high. These results clearly indicate that distortions of the molecular skeleton of the solute species due to its interactions with the solvent molecules is a dominant factor that affects the experimentally observed solvatochromism. Nonetheless, classical sampling does not correctly capture these structurally subtle distortions, which yet have a significant impact on the excited-state electronic structure, although pronounced NQEs on indole-water hydrogen bonding in solution are not observed (see Figure S3). Once the solvent molecules are considered in addition, the calculated spectrum based on PIQTB quantum sampling qualitatively matches the measured one also in the positions of the band maxima in the energy window below 5.1 eV. Furthermore, the increase of the absorbance starting at about 5.14 eV is reproduced only when both the impact of NQEs on the solute structure and the solvent impact on the local electronic structure are considered.

The above results unambiguously prove that both the distortions of the solute molecule caused by solvent fluctuations and the changes in its excited states in solution contribute substantially to the total solvent effect on UV/Vis spectra in aqueous solution. The effects by the former structural factor are accurately reproduced only in sampling Schemes that rigorously take account of the quantum-thermal fluctuations in the liquid state, such as PIQTB, whereas those by excited-state electronic structure are already described for the $^1\pi\pi^*$ transitions of indole with sufficient accuracy by an implicit solvation model. Nevertheless, we emphasize that such good performance of simple continuum solvation models such as COSMO can be expected only when the dominant NTOs do not reach into the region of hydrogen bonds. In such a regime, explicitly hydrogen-bonded water molecules are involved in the dominant NTOs of the electronic transitions (see Tables S3, S4 and Figure S7). We finally note that NQEs also increase the degree of level inversion between ^1L_b and ^1L_a upon solvation. Further details of this are given in Section 2.5 of the Supporting Information.

In summary, we have calculated the UV/Vis absorption spectra of indole in the gas phase and in aqueous solution with a focus on assessing the importance of nuclear quantum effects on the experimental spectra. The present calculations of the electronic excitations are based on an accurate wavefunction-based approach, which avoids any scaling or shifting of excitation energies. The key finding is that purely thermal fluctuations, as obtained from molecular dynamics with classical nuclei, are insufficient to reproduce either the proper positioning of the bands or the overall lineshape of the UV/Vis absorption spectrum in solution. Only after considering quantum-statistical fluctuations in the aqueous solution at ambient conditions obtained from path integral simulations that quantize the motion of all nuclei in the system, good agreement between the calculated and measured UV/Vis spectra is achieved—concerning not only the band widths but also the magnitude of the solvatochromic shifts. The general conclusion is therefore that the effects of quantized nuclear motion are clearly "visible" in UV/Vis spectra of such chromophores in aqueous solution and, thus, must be included in calculations if one aims for predictive accuracy.

Acknowledgements

This research was funded by the Deutsche Forschungsgemeinschaft (DFG, German Research Foundation) under Germany's Excellence Strategy—EXC 2033—390677874—RESOLV as well as by the individual DFG grant to D. M. (MA 1547/11-2). This research was also supported by the Alexander von Humboldt Foundation through a Research Fellowship to S. T. (JPN 1201668 HFST-P). Computing resources were provided by LRZ (SuperMUC-NG) as well as by HPC@ZEMOS, HPC-RESOLV, and BOVILAB@-

© 2024 Wiley-VCH GmbH

15213773, 2025, 3, Downloaded from https://onlinelibrary.wiley.com/doi/10.1002/anie.202416058 by Ruhr-Universität Bochum, Wiley Online Library on [05/03/2025]. See the Terms and Conditions (https://onlinelibrary.wiley.com/terms-and-conditions) on Wiley Online Library for rules of use; OA articles are governed by the applicable Creative Commons License

RUB. We thank W. Dawson and B. Cooper for proofreading.

Conflict of Interest

The authors declare no competing financial interest.

Data Availability Statement

The data that support the findings of this study are openly available in RESOLVdata at https://doi.org/10.17877/RESOLV-2024-m2kiewcc, reference number [90].

Keywords: UV/Vis spectroscopy · solvent effects · solvatochromism · path integral simulations · ab initio calculations

[1] C. Reichardt, T. Welton, *Solvents and Solvent Effects in Organic Chemistry*, 4th ed., Wiley-VCH, Weinheim, **2011**.
[2] C. Reichardt, *J. Org. Chem.* **2022**, *87*, 1616.
[3] I. Benjamin, *Chem. Rev.* **2006**, *106*, 1212.
[4] J. Dong, K. M. Solntsev, L. M. Tolbert, *J. Am. Chem. Soc.* **2006**, *128*, 12038.
[5] F. Würthner, G. Archetti, R. Schmidt, H.-G. Kuball, *Angew. Chem. Int. Ed.* **2008**, *47*, 4529.
[6] R. W. Sinkeldam, N. J. Greco, Y. Tor, *Chem. Rev.* **2010**, *110*, 2579.
[7] A. Marini, A. Muñoz-Losa, A. Biancardi, B. Mennucci, *J. Phys. Chem. B* **2010**, *114*, 17128.
[8] R. Pardo, M. Zayat, D. Levy, *Chem. Soc. Rev.* **2011**, *40*, 672.
[9] R. N. Dsouza, U. Pischel, W. M. Nau, *Chem. Rev.* **2011**, *111*, 7941.
[10] H. Kim, M. Cho, *Chem. Rev.* **2013**, *113*, 5817.
[11] S. B. Nielsen, M. B. Nielsen, A. Rubio, *Acc. Chem. Res.* **2014**, *47*, 1417.
[12] A. Petrone, G. Donati, P. Caruso, N. Rega, *J. Am. Chem. Soc.* **2014**, *136*, 14866.
[13] A. Arjona-Esteban, M. Stolte, F. Würthner, *Angew. Chem. Int. Ed.* **2016**, *55*, 2470.
[14] A. S. Klymchenko, *Acc. Chem. Res.* **2017**, *50*, 366.
[15] C. A. Hoelzel, H. Hu, C. H. Wolstenholme, B. A. Karim, K. T. Munson, K. H. Jung, H. Zhang, Y. Liu, H. P. Yennawar, J. B. Asbury, X. Li, X. Zhang, *Angew. Chem. Int. Ed.* **2020**, *59*, 4785.
[16] W. R. Kitzmann, K. Heinze, *Angew. Chem. Int. Ed.* **2023**, *62*, e202213207.
[17] M. Homocianu, *Microchem. J.* **2024**, *198*, 110166.
[18] M. Glasbeek, H. Zhang, *Chem. Rev.* **2004**, *104*, 1929.
[19] F. Buchner, A. Nakayama, S. Yamazaki, H.-H. Ritze, A. Lübcke, *J. Am. Chem. Soc.* **2015**, *137*, 2931.
[20] A. Rondi, Y. Rodriguez, T. Feurer, A. Cannizzo, *Acc. Chem. Res.* **2015**, *48*, 1432.
[21] T. Kumpulainen, B. Lang, A. Rosspeintner, E. Vauthey, *Chem. Rev.* **2017**, *117*, 10826.
[22] R. Borrego-Varillas, D. C. Teles-Ferreira, A. Nenov, I. Conti, L. Ganzer, C. Manzoni, M. Garavelli, A. Maria de Paula, G. Cerullo, *J. Am. Chem. Soc.* **2018**, *140*, 16087.
[23] B. Dereka, D. Svechkarev, A. Rosspeintner, A. Aster, M. Lunzer, R. Liska, A. M. Mohs, E. Vauthey, *Nat. Commun.* **2020**, *11*, 1925.
[24] A. Aster, F. Zinna, C. Rumble, J. Lacour, E. Vauthey, *J. Am. Chem. Soc.* **2021**, *143*, 2361.
[25] R. Kusaka, S. Nihonyanagi, T. Tahara, *Nat. Chem.* **2021**, *13*, 306.
[26] R. K. Venkatraman, A. J. Orr-Ewing, *Acc. Chem. Res.* **2021**, *54*, 4383.
[27] R. Borrego-Varillas, A. Nenov, P. Kabaciński, I. Conti, L. Ganzer, A. Oriana, V. K. Jaiswal, I. Delfino, O. Weingart, C. Manzoni, I. Rivalta, M. Garavelli, G. Cerullo, *Nat. Commun.* **2021**, *12*, 7285.
[28] C. J. C. Jordan, E. A. Lowe, J. R. R. Verlet, *J. Am. Chem. Soc.* **2022**, *144*, 14012.
[29] Y. Miura, Y.-i. Yamamoto, S. Karashima, N. Orimo, A. Hara, K. Fukuoka, T. Ishiyama, T. Suzuki, *J. Am. Chem. Soc.* **2023**, *145*, 3369.
[30] Y.-P. Chang, T. Balciunas, Z. Yin, M. Sapunar, B. N. C. Tenorio, A. C. Paul, S. Tsuru, H. Koch, J.-P. Wolf, S. Coriani, H. J. Wörner, *Nat. Phys.* **2024** DOI: 10.1038/s41567-024-02703-w.
[31] V. Barone, R. Improta, N. Rega, *Acc. Chem. Res.* **2008**, *41*, 605.
[32] D. Loco, N. Gelfand, S. Jurinovich, S. Protti, A. Mezzetti, B. Mennucci, *J. Phys. Chem. A* **2018**, *122*, 390.
[33] J. J. Nogueira, L. González, *Annu. Rev. Phys. Chem.* **2018**, *69*, 473.
[34] T. J. Zuehlsdorff, C. M. Isborn, *Int. J. Quantum Chem.* **2019**, *119*, e25719.
[35] M. Eskandari, J. C. Roldao, J. Cerezo, B. Milián-Medina, J. Gierschner, *J. Am. Chem. Soc.* **2020**, *142*, 2835.
[36] J. Chen, B. Chan, Y. Shao, J. Ho, *Phys. Chem. Chem. Phys.* **2020**, *22*, 3855.
[37] S. Gómez, T. Giovannini, C. Cappelli, *Phys. Chem. Chem. Phys.* **2020**, *22*, 5929.
[38] U. Raucci, F. Perrella, G. Donati, M. Zoppi, A. Petrone, N. Rega, *J. Comput. Chem.* **2020**, *41*, 2228.
[39] S. Abou-Hatab, V. Carnevale, S. Matsika, *J. Chem. Phys.* **2021**, *154*, 064104.
[40] S. Tsuru, B. Sharma, M. Nagasaka, C. Hättig, *J. Phys. Chem. A* **2021**, *125*, 7198.
[41] A. Manian, R. A. Shaw, I. Lyskov, S. P. Russo, *Phys. Chem. Chem. Phys.* **2022**, *24*, 3357.
[42] D. Valverde, S. Mai, S. Canuto, A. C. Borin, L. González, *JACS Au* **2022**, *2*, 1699.
[43] S. Tsuru, B. Sharma, D. Marx, C. Hättig, *J. Chem. Theory Comput.* **2023**, *19*, 2291.
[44] A. Arcidiacono, E. Cignoni, P. Mazzeo, L. Cupellini, B. Mennucci, *J. Phys. Chem. A* **2024**, *128*, 3646.
[45] F. Della Sala, R. Rousseau, A. Görling, D. Marx, *Phys. Rev. Lett.* **2004**, *92*, 183401.
[46] M. Barbatti, K. Sen, *Int. J. Quantum Chem.* **2016**, *116*, 762.
[47] C. Pieroni, F. Becuzzi, L. Creatini, G. Granucci, M. Persico, *J. Chem. Theory Comput.* **2023**, *19*, 2430.
[48] O. Svoboda, M. Ončák, P. Slavíček, *J. Chem. Phys.* **2011**, *135*, 154301.
[49] Y. K. Law, A. A. Hassanali, *J. Phys. Chem. A* **2015**, *119*, 10816.
[50] D. Hollas, E. Muchová, P. Slavíček, *J. Chem. Theory Comput.* **2016**, *12*, 5009.
[51] Y. K. Law, A. A. Hassanali, *J. Chem. Phys.* **2018**, *148*, 102331.
[52] J. P. Zobel, M. Heindl, J. J. Nogueira, L. González, *J. Chem. Theory Comput.* **2018**, *14*, 3205.
[53] D. Berta, D. Ferenc, I. Bakó, Á. Madarász, *J. Chem. Theory Comput.* **2020**, *16*, 3316.
[54] A. Borrego-Sánchez, M. Zemmouche, J. Carmona-García, A. Francés-Monerris, P. Mulet, I. Navizet, D. Roca-Sanjuán, *J. Chem. Theory Comput.* **2021**, *17*, 3571.
[55] P. P. Fehér, Á. Madarász, A. Stirling, *J. Chem. Theory Comput.* **2021**, *17*, 6340.
[56] L. Turi, B. Baranyi, Á. Madarász, *J. Chem. Theory Comput.* **2024**, *20*, 4265.

© 2024 Wiley-VCH GmbH

15213773, 2025, 3, Downloaded from https://onlinelibrary.wiley.com/doi/10.1002/anie.202416058 by Ruhr-Universität Bochum, Wiley Online Library on [05/03/2025]. See the Terms and Conditions (https://onlinelibrary.wiley.com/terms-and-conditions) on Wiley Online Library for rules of use; OA articles are governed by the applicable Creative Commons License

[57] T. J. Zuehlsdorff, J. A. Napoli, J. M. Milanese, T. E. Markland, C. M. Isborn, *J. Chem. Phys.* **2018**, *149*, 024107.
[58] T. J. Zuehlsdorff, S. V. Shedge, S.-Y. Lu, H. Hong, V. P. Aguirre, L. Shi, C. M. Isborn, *Annu. Rev. Phys. Chem.* **2021**, *72*, 165.
[59] M. S. Chen, Y. Mao, A. Snider, P. Gupta, A. Montoya-Castillo, T. J. Zuehlsdorff, C. M. Isborn, T. E. Markland, *J. Phys. Chem. Lett.* **2023**, *14*, 6610.
[60] M. Ceriotti, W. Fang, P. G. Kusalik, R. H. McKenzie, A. Michaelides, M. A. Morales, T. E. Markland, *Chem. Rev.* **2016**, *116*, 7529.
[61] R. J. Sundberg, *Indoles*, Academic Press, London, **1996**.
[62] V. Sharma, P. Kumar, D. Pathak, *J. Heterocycl. Chem.* **2010**, *47*, 491.
[63] J.-H. Lee, J. Lee, *FEMS Microbiol. Rev.* **2010**, *34*, 426.
[64] D. F. Taber, P. K. Tirunahari, *Tetrahedron* **2011**, *67*, 7195.
[65] S. M. O'Mahony, G. Clarke, Y. E. Borre, T. G. Dinan, J. F. Cryan, *Behav. Brain Res.* **2015**, *277*, 32.
[66] N. Gupta, D. Goyal, *Chem. Heterocycl. Compd.* **2015**, *51*, 4.
[67] Q. Ma, X. Zhang, Y. Qu, *Front. Microbiol.* **2018**, *9*, 2625.
[68] P. V. Thanikachalam, R. K. Maurya, V. Garg, V. Monga, *Eur. J. Med. Chem.* **2019**, *180*, 562.
[69] M. A. Pappolla, G. Perry, X. Fang, M. Zagorski, K. Sambamurti, B. Poeggeler, *Neurobiol. Dis.* **2021**, *156*, 105403.
[70] R. Livingstone, O. Schalk, A. E. Boguslavskiy, G. Wu, L. T. Bergendahl, A. Stolow, M. J. Paterson, D. Townsend, *J. Chem. Phys.* **2011**, *135*, 194307.
[71] G. Kumar, A. Roy, R. S. McMullen, S. Kutagulla, S. E. Bradforth, *Faraday Discuss.* **2018**, *212*, 359.
[72] S. T. Park, A. Gahlmann, Y. He, J. S. Feenstra, A. H. Zewail, *Angew. Chem. Int. Ed.* **2008**, *47*, 9496.
[73] T. J. Godfrey, H. Yu, M. S. Biddle, S. Ullrich, *Phys. Chem. Chem. Phys.* **2015**, *17*, 25197.
[74] M. M. Zawadzki, J. O. F. Thompson, E. A. Burgess, M. J. Paterson, D. Townsend, *Phys. Chem. Chem. Phys.* **2015**, *17*, 26659.
[75] D. Marx, J. Hutter, *Ab Initio Molecular Dynamics: Basic Theory and Advanced Methods*, Cambridge University Press, Cambridge, **2009**.
[76] F. Brieuc, H. Dammak, M. Hayoun, *J. Chem. Theory Comput.* **2016**, *12*, 1351.
[77] C. Schran, F. Brieuc, D. Marx, *J. Chem. Theory Comput.* **2018**, *14*, 5068.
[78] J. Schirmer, *Phys. Rev. A* **1982**, *26*, 2395.
[79] J. Schirmer, *Phys. Rev. A* **1991**, *43*, 4647.
[80] C. Hättig, *Adv. Quantum Chem.* **2005**, *50*, 37.
[81] P.-F. Loos, A. Scemama, D. Jacquemin, *J. Phys. Chem. Lett.* **2020**, *11*, 2374.
[82] A. V. Luzanov, A. A. Sukhorukov, V. É. Umanskii, *Theor. Exp. Chem.* **1976**, *10*, 354.
[83] A. V. Luzanov, O. A. Zhikol, in *Practical Aspects of Computational Chemistry I: An Overview of the Last Two Decades and Current Trends* (Eds.: J. Leszczynski, M. K. K. Shukla), Springer, Heidelberg, **2012**, pp. 415–449.
[84] R. L. Martin, *J. Chem. Phys.* **2003**, *118*, 4775.
[85] I. Mayer, *Chem. Phys. Lett.* **2007**, *437*, 284.
[86] J. R. Platt, *J. Chem. Phys.* **1949**, *17*, 484.
[87] A. Klamt, G. Schüürmann, *J. Chem. Soc. Perkin Trans.* **1993**, *2*, 799.
[88] S. Karbalaei Khani, A. Marefat Khah, C. Hättig, *Phys. Chem. Chem. Phys.* **2018**, *20*, 16354.
[89] J. Catalán, *Phys. Chem. Chem. Phys.* **2015**, *17*, 12515.
[90] [dataset] C. Hättig, **2024**, *Raw data for: "Nuclear Quantum Effects Have a Significant Impact on UV/Vis Absorption Spectra of Chromophores in Water"*, *RESOLVdata* DOI: 10.17877/RESOLV-2024-m2kiewcc.

Manuscript received: August 21, 2024
Accepted manuscript online: October 30, 2024
Version of record online: December 10, 2024

© 2024 Wiley-VCH GmbH

15213773, 2025, 3, Downloaded from https://onlinelibrary.wiley.com/doi/10.1002/anie.202416058 by Ruhr-Universität Bochum, Wiley Online Library on [05/03/2025]. See the Terms and Conditions (https://onlinelibrary.wiley.com/terms-and-conditions) on Wiley Online Library for rules of use; OA articles are governed by the applicable Creative Commons License